Effects of arousal and movement on secondary somatosensory and visual thalamus

Gordon H. Petty[1], Amanda K. Kinnischtzke[1], Y. Kate Hong, and Randy M. Bruno[2]

Dept. of Neuroscience, Columbia University, New York, NY, 10027 USA

Kavli Institute for Brain Science, Columbia University, New York, NY, 10027 USA

Zuckerman Mind Brain Behavior Institute, Columbia University, New York, NY, 10027 USA

1 These authors contributed equally.

2 Corresponding Author:

Randy M. Bruno
3227 Broadway
Room L7-008, Mail Code
New York, NY 10027
Phone: 212-853-1044
Email: randybruno@columbia.edu

Summary

All neocortical sensory areas have an associated primary and secondary thalamic nucleus. While the primary nuclei encode sensory information and relay it to cortex, the drivers of activity in secondary nuclei are poorly understood. We recorded juxtasomally from neurons in secondary somatosensory (POm) and visual (LP) thalamic nuclei of awake head-fixed mice with simultaneous whisker tracking and pupilometry. POm activity correlated with the slow components of whisker movement but not fast precise kinematics. This movement modulation was not due to sensory reafference, persisting after unilateral paralysis of the whisker pad. POm tracked whisking even more strongly after optogenetic silencing of primary somatosensory and motor cortex, indicating that cortical motor efference copy cannot explain movement modulation. We observed that whisking and pupil dilation were strongly correlated, raising the possibility that POm tracks arousal rather than whisker movement. LP, being part of the visual system, is not expected to encode whisker movement. However, we discovered that LP and POm track whisking equally well, suggesting a global arousal effect on both nuclei. Our results suggest that motor signals are largely absent in POm. We conclude that global arousal may be a prominent modulator of secondary thalamic nuclei.

Introduction

Somatosensory, visual, auditory, and gustatory cortex are each reciprocally connected with a specific subset of thalamic nuclei. These nuclei can be subdivided into primary and secondary (often termed “higher-order”) nuclei (Herkenham, 1980; Guillery and Sherman, 2002; Phillips *et al.*, 2019). The primary nuclei are the main source of sensory input to the cortex and respond robustly to sensory stimulation with low latency (Chiaia *et al.*, 1991; Sherman and Guillery, 2002; Wimmer *et al.*, 2010; Constantinople and Bruno, 2013). Unlike primary nuclei, the secondary nuclei are interconnected with many cortical and subcortical regions, and their role in sensation and cognition is poorly understood.

In rodents, the facial whisker representation of primary somatosensory cortex (S1) is tightly integrated with two thalamic nuclei: the ventral posteromedial nucleus (VPM) and the posterior medial nucleus (POm). Compared to the primary nucleus VPM, the secondary nucleus POm has broader receptive fields, longer-latency sensory responses, and poorly encodes fine aspects of whisker touch such as contact timing and stimulus frequency (Diamond *et al.*, 1992; Moore, 2004; Masri *et al.*, 2008; Moore *et al.*, 2015). It receives input from S1, motor cortex, posterior parietal cortex, the zona incerta, and many other subcortical regions in addition to brainstem afferents (Chiaia *et al.*, 1991; Trageser and Keller, 2004; Olsen and Witter, 2016). Whereas VPM innervates cortical layer 4 and the border of layers 5B and 6, POm projects to the apical dendrites of layer 1 as well as layer 5A (Wimmer *et al.*, 2010). POm is a stronger driver of layer 2/3 cells than cortico-cortical synapses and can enhance sensory responses in pyramidal neurons of layers 2/3 and 5 (Mease, Metz and Groh, 2016; Zhang and Bruno, 2019). It is thus positioned to strongly influence sensory computations in S1. However, what POm activity ultimately encodes remains a mystery.

One possibility is that POm preferentially responds to self-generated movements, through either sensory reafference or motor efference copy, rather than extrinsic tactile sensations (Yu *et al.*, 2006). Recent studies in awake animals have observed that POm encodes whisker motion and contact less well than VPM does (Moore *et al.*, 2015; Urbain *et al.*, 2015), which raises the question of why a secondary pathway would be needed to encode self-generated motion. Several labs have noted that a subset of POm neurons are activated by pain (Masri *et al.*, 2009; Frangeul *et al.*, 2014), a powerful stimulus for directing behavioral state. More subtle forms of behavioral state changes are found in primate secondary visual thalamus (lateral pulvinar), which has been implicated repeatedly in mediating attention (Petersen, Robinson and Morris, 1987; Wilke *et al.*, 2010; Saalmann *et al.*, 2012).

The rodent homolog to the pulvinar (lateral posterior nucleus, LP) is active during mismatch of movement and visual stimuli (Roth *et al.*, 2016), which might reflect elevations in global arousal or visual attention. These results raise the possibility that all secondary nuclei are strongly modulated by changes in behavioral state.

Here we investigate how cortical and sensory inputs influence POm activity in the awake mouse. We further examine how POm activity compares to that of LP to investigate general principles of secondary thalamus function.

Results

Initially, we characterized the degree to which POm encodes whether or not an animal is whisking versus the fine details of movements. We recorded juxtasomally from single neurons in head-fixed mice while acquiring high-speed video of the contralateral whisker field, from which whisker positions could be algorithmically extracted (Figure 1A, B; 22 POm neurons in 5 mice). To measure slow aspects of whisking, we calculated whisking amplitude from the median angle of all whiskers. Whisking amplitude is defined as the difference in angle between set-point and protraction over the whisking cycle (Hill *et al.*, 2011; Moore *et al.*, 2015, see Methods). Whisking amplitude was then used to determine periods of whisking and quiescence. Whisking bouts were defined as periods of time when whisking amplitude exceeded 20% of the maximum for more than 250 msec (Figure 1B, shaded areas).

Whisking substantially elevated POm firing rates. We computed the mean firing rate for each cell during periods when the mouse was whisking and quiescent (Figure 1C). The firing rates of POm cells were significantly higher during bouts of whisking, with a mean increase of 4.6Hz, or 133% ($p < 10^{-4}$, paired t-test). To understand which components of whisking might drive POm activity, we calculated the cross-correlation between POm firing rate and three features of whisking activity: the median angle (Figure 1D, gray), the amplitude metric which captures the slow envelope of whisking (green), and the median angle bandpass-filtered from 4-30 Hz (black), which reflects fast individual protractions and retractions of the whisker. We found little correlation with the bandpass-filtered angle, while both whisker angle and whisking amplitude had prominent correlations centered around t = 0. The strongest correlate with POm activity was whisking amplitude, suggesting that POm is coupled only to the slow components of whisking.

To further investigate the encoding of the fast components of whisking in POm, we performed an analysis of phase coding during whisking bouts. A Hilbert transform was applied to the bandpass-filtered median whisker angle to quantify phase precisely. We identified the phase at which each action potential occurred during whisking and plotted distributions of firing rate as a function of phase. For each cell, we fit a sinusoid to characterize the cell's preferred phases (the phase of the whisk cycle that elicited the highest firing rate) and modulation depth (the degree to which phase impacts firing rate, measured as the peak-trough difference normalized by mean firing rate). Figure 1E shows the phase relationship of two example cells: one with significant coding (top) and the other insignificant (bottom). Most POm cells (19/22) resembled the non-phase coding example, having little or no modulation (right). Together, these results indicate that a large majority of POm cells do not encode fast whisking dynamics such as whisker angle or whisk cycle phase. Rather, they track slow components of whisking, *i.e.* the difference between whisking and quiescence.

One possible source of whisking-related activity is reafferent sensory input: when the mouse whisks, the movement could deform the whisker follicle and stimulate mechanoreceptors. To measure the degree to which POm activity is driven by the sensory reafference caused by whisking, we severed

the facial motor nerve on the right side of the face, contralateral to our recordings, while taking video of the left (ipsilateral) side of the face (Figure 2A). Mice were no longer able to move the right whisker pad, while the whisking on the left side of the face was unaffected (Figure 2B). Without whisker movement, there can be no reafferent sensory input from the right whisker pad. As in intact mice, firing rates of POm neurons in nerve cut animals were significantly higher during whisking bouts (Figure 2C, n = 12, p = 0.00068, paired t test) and to a similar degree (mean increase of 4.8Hz, or 51%). POm firing rates also correlated with ipsilateral whisking amplitude at a similar magnitude and with a similar lag as in the contralateral whisker field in intact mice (Figure 2D). This demonstrates that the correlation of POm activity and whisking is not due to ascending reafferent information.

POm is reciprocally connected to several cortical areas, potentially making cortical input a strong driver of POm activity (Chiaia *et al.*, 1991; Diamond *et al.*, 2008; Mease, Metz and Groh, 2016). In particular, input from S1 and primary motor cortex (M1) could convey sensorimotor information, such as a motor efference copy, that would drive whisking-related activity independent of ascending sensory input. To test this, we expressed halorhodopsin in all excitatory cortical neurons by crossing Emx1-Cre mice with a Cre-condition halorhodopsin responder line. We recently demonstrated that this technique could block 95-100% of action potentials throughout all cortical layers of awake behaving mice (Hong *et al.* 2018). We recorded from POm cells and, for comparison, VPM cells while silencing S1 or M1 with an amber laser.

M1 silencing reduced the baseline firing rate of POm cells, but POm activity was still elevated during whisking regardless of whether the laser was on or off (Figure 3A, left). Interestingly, silencing M1 also resulted in an increased correlation between POm firing rate and whisking amplitude (right). Silencing M1, which does not directly project to VPM, changed neither VPM firing rates nor the correlation of VPM activity and whisking amplitude (Figure 3C).

In parallel S1 experiments, silencing reduced POm activity, both when mice were whisking and quiescent (Figure 3B, left). Similar to the effect of M1 silencing, this again resulted in an increase in the correlation between POm activity and whisking amplitude (right). There was a tendency for S1 inhibition to reduce overall activity in VPM, perhaps reflecting known corticothalamic connections between S1 and VPM, but this effect did not reach significance (Figure 3D; p = 0.1). Silencing S1 did not impact the correlation of VPM spiking and whisking. These results demonstrate that POm is not inheriting information about whisking amplitude from M1 or S1. Rather, corticothalamic inputs appear to transmit signals other than whisker movements, effectively creating noise in POm activity that reduces its correlation with whisking amplitude.

Neither reafference nor cortical sources of motor efference copy explain the presence of movement signals in POm. This raises the question of whether POm encodes movement at all. One possibility is that the coupling of POm spiking and whisking is due to POm encoding another variable that is tightly locked to whisking, such as arousal. To investigate this, we measured pupil diameter as a metric of arousal. We acquired videos of the pupil and whiskers while recording from POm (Figure 4A). Pupil diameter was tightly correlated with whisking, with a peak correlation of 0.39 with pupil dilation lagging whisking amplitude by 880 msec (Figure 4B). Pupil diameter also correlated with POm activity, to a similar degree as whisking, but with a lag of 950 msec (Figure 4C).

We reasoned that, if the modulation of POm by whisking was truly due to whisker movement rather than a collinear variable, other secondary thalamic nuclei would not be expected to track whisking. The secondary visual thalamic nucleus LP is the rodent homolog of the primate lateral pulvinar. LP is primarily coupled with cortical and subcortical visual areas (Nakamura *et al.*, 2015), rather than somatosensory ones. Because of their different connectivity, POm and LP are expected to carry separate sensorimotor signals related to somatosensation and vision, respectively. Therefore, LP

would not be expected to encode whisker movement. By contrast, changes in behavioral state, such as overall animal arousal as suggested by our pupil measurements, might modulate all thalamic nuclei, including LP and POm.

We tested this idea by recording juxtasomally from LP (Figure 5A, B; 29 cells from 4 mice). Surprisingly, we found that LP activity was significantly increased during whisking bouts (Figure 5C, increase of 5.04Hz, 42.6%, $p < 10^{-4}$, paired t test). Like POm, LP activity correlated with both whisking amplitude and median whisker angle with low latency (Figure 5D). Since changes in pupil diameter will cause more light to fall on the retina, the LP correlation with whisking might be an artifact of pupil dilation. To control for this, a subset of cells were recorded in low light. Under these darker conditions, the pupil was maximally dilated and did not change (Figure 5B), rendering input to the retina largely constant. However, these cells still showed an equivalent increase in firing rate during whisking (Figure 5C, orange). Thus, LP activity appears to track whisking independent of changes in visual input, which suggests that the effect in both nuclei is due to arousal-whisking collinearity rather than a direct effect of whisking.

Together, our results indicate that the slow component of whisking-related activity in POm is neither a result of ascending motion signals from reafferent mechanisms nor of descending corticothalamic efferent mechanisms. We conclude instead that arousal may strongly dictate the activity of secondary thalamic nuclei, including POm and LP.

Discussion

We aimed to characterize how the secondary somatosensory thalamus encodes features of whisker motion. Juxtasomal recordings of POm cells revealed that the region mainly tracks slow components of whisking. Consistent with previous studies (Moore *et al.*, 2015; Urbain *et al.*, 2015), mouse POm firing rates are much higher during bouts of whisking compared to when a mouse is quiescent. Further, POm activity correlates with the slow change in whisking amplitude but not with the fast changes of the whisk cycle. Only a small fraction (~14%) of our POm cells encoded whisking phase. We have demonstrated that these effects are not due to sensory reafference from self-generated movements, as transection of the facial motor nerve did not decorrelate POm activity and ipsilateral whisking. We also showed that cortical inputs do not underlie whisking modulation of POm, as both S1- and M1-silencing enhanced the correlation between POm spiking and whisking amplitude. What appears to be whisking-related activity in POm is likely instead a consequence of the encoding of behavioral state. This effect may be a general property of all secondary thalamic nuclei, as we observed identical whisking-related activity in the secondary visual thalamus LP. Future studies are needed to examine if this principle holds in some auditory thalamic subnuclei and perhaps even thalamic nuclei connected to motor cortex and other frontal areas.

The paralemniscal system has been speculated to be a parallel secondary afferent pathway (Yu *et al.*, 2006; Frangeul *et al.*, 2014). In anesthetized rats, POm does not appear to be sensitive to fine aspects of whisker touch, having very large receptive fields and long-latency responses (Diamond *et al.*1998*,* Trageser *et al.* 2004). One might expect that very large synchronized movements of the whiskers, such as during whisking, would elicit a response from POm. However, paralyzing the face produces no change in the correlation between POm activity and ipsilateral whisking amplitude (Figure 2). Interestingly, mouse barrel cortex is also modulated by whisking and quiescence in absence of sensory input: whisking is associated with a decrease in synchrony between layer 2/3 pyramidal cells in S1 and an increase in discharges by VPM, which is unaltered by bilateral transection of the infraorbital nerve sensory nerve (Poulet and Petersen, 2008). Manipulations of somatosensory thalamus strongly impacted cortical synchronization (Poulet *et al.*, 2012). Our results show that both

POm and LP correlate with movement/arousal. Further studies are needed to determine if cortical synchronization is determined by inputs from VPM, POm, or both.

POm receives descending input from many cortical regions including M1 and S1. Conceivably these inputs could modulate ascending sensory input or provide the thalamus with a motor efference copy (Mease, Metz and Groh, 2016; Sherman, 2016). Similarly, LP and LGN axons in V1 exhibit eye movement related signals (Roth *et al.*, 2016). Previous studies in anesthetized rats have shown that cortical inactivation will silence POm, but not VPM (Diamond 1992). Therefore, cortex might be the primary source of excitatory input to POm. However, we discovered that, in the awake mouse, silencing either M1 or S1 only slightly reduces the firing rate of POm cells and has little to no effect on VPM activity (Figure 3). We conclude that, while S1 and M1 provide significant excitatory inputs to POm, these inputs are not the sole or primary drivers of POm activity. Moreover, silencing increased rather than decreased the correlation between POm activity and whisking amplitude. If POm activity were primarily representative of a cortical efference copy, we would expect the opposite effect. While we cannot rule out the possibility that POm receives some efference copy from cortex, such input is not the cause of what at first appears to be whisking modulation. POm might instead be under equal or greater control of subcortical regions such as trigeminal brainstem complex, zona incerta, the thalamic reticular nucleus, and neuromodulatory brainstem centers – all of which receive inputs from broad areas of the nervous system (Pinault and Deschênes, 1998; Trageser and Keller, 2004).

As POm continues to track whisking in absence of both ascending sensory input and descending cortical input, we propose that the activity we observe is not sensorimotor in nature, but rather representative of thalamic coding of internal state. POm axons project to the apical dendrites of pyramidal cells (Meyer *et al.*, 2010; Wimmer *et al.*, 2010), where they might drive state-dependent changes in activity and synchrony. Arousal is one of the simpler internal states, which we and others have previously shown has dramatic effects on cortical dynamics (Constantinople and Bruno, 2011; Reimer *et al.*, 2014; Vinck *et al.*, 2015). We observed that whisking and pupil diameter, which closely tracks arousal, are highly correlated with each other. Due to the collinearity between pupil and whisking dynamics, they both correlate with POm firing rates (Figure 4C). To dissect out arousal and movement, we took the novel approach of comparing these dynamics to those of LP, the rodent homolog of the primate lateral pulvinar. We found a near-identical relationship with whisking in LP as we observed in POm (Figure 5), despite the fact that there is no known connectivity between LP and the whisker system. Like POm, these responses do not appear to be sensory dependent, as they persist even in low-light conditions where the pupil is maximally dilated and can no longer contribute to changes in retinal activity. If this state-dependent modulation of secondary thalamic nuclei is not sensory reafference or derived from S1 or M1, likely candidates would include a large number of neuromodulators. For instance, zona incerta terminals within POm are regulated by acetylcholine (Masri *et al.*, 2006) and are likely modulated in the same way in LP. However, acetylcholine and norepinephrine both track pupil dynamics (Reimer *et al.*, 2016) and are also plausible culprits. In addition to these two well-studied modulators there are many others known to have function in thalamus (Varela, 2014). Furthermore, any of these modulators could act directly on POm and LP or indirectly through ZI, TRN, brainstem nuclei, or other inputs.

This arousal effect we have described may be a more general version of modality-specific attentional effects that have been proposed for at least some secondary thalamic nuclei. In primates, pulvinar neurons respond strongest when stimuli are presented in attended regions of visual space (Petersen, Robinson and Keys, 1985), and lesion of the pulvinar leads to deficits of selective attention during visual tasks (Ward *et al.*, 2002; Wilke *et al.*, 2010). Human patients with pulvinar damage exhibit spatial neglect, in which a stimulus can be perceived normally in isolation but is missed or distorted in the presence of neighboring stimuli (Karnath, Himmelbach and

Rorden, 2002; Snow *et al.*, 2009). By analogy, one might hypothesis that POm provides feedback that selects somatosensory stimuli for further cortical processing. This selective attention within a modality could be a general principle of secondary thalamic function.

Elevated firing rates in secondary thalamus due to arousal or attention could be useful for creating periods of heightened cortical plasticity. Recent studies have shown that repetitive sensory stimuli in anesthetized animals drives POm input to pyramidal neurons, which leads to enhancement of future sensory responses in cortex (Gambino *et al.*, 2014). A potential mechanism of this is that disinhibition of apical dendritic spikes leads to long-term potentiation of local recurrent synapses among cortical pyramidal neurons (Williams and Holtmaat, 2019). Furthermore, an *in vivo* study found that associative learning can also potentiate long-range POm connections onto pyramidal neurons when subsequently measured *in vitro* (Audette *et al.*, 2019). Future studies are needed to address the links between arousal, attention, and plasticity.

Acknowledgments

The authors thank S. Benezra and G. Pierce for comments on the manuscript and D. Baughman for technical support.

Author Contributions

Conceptualization: AKK and RMB; Investigation: AKK and GHP; Formal Analysis: AKK, GHP, and RMB; Optogenetics Methodology and Resources: YKH; Writing: GHP and RMB.

Declaration of Interests

The authors declare no competing interests.

Figure titles and legends

Figure 1. POm cells mainly track slow components of whisking activity. (A) An example frame from a video, captured at 125 FPS. Identified whiskers are highlighted in green, and whisker bases are indicated by yellow circles. **(B)** Example traces of juxtasomal POm recording and whisking. The median angle of all whiskers in each video frame (middle, gray) was used to calculate the whisking amplitude (bottom, green). Whisking events (green shaded areas) were defined as those periods where whisking amplitude exceeded 20% of maximum for at least 250 msec. **(C)** Scatter plot of POm firing rates during whisking and quiescence (n = 22 putative POm cells, 5 mice, mean increase of 4.6Hz, or 133%, $p < 10^{-4}$, paired t-test). *Green*, cell in B. (**D)** Cross-correlation of POm firing rate and whisking amplitude (green), angle (gray), and 4-30 Hz bandpass-filtered angle (black). Shading, SEM. **(E)** *Left,* Firing rate as a function of phase in the whisking cycle for two example POm units. A sinusoid model (black) was fit to each cell and used to calculate preferred phase (white markers) and modulation depth. *Right,* A polar plot of modulation depth (radius) and preferred phase (angle) of each POm unit. *Filled circles*, cells with significant phase modulation ($p<0.05$, Kuiper test, Bonferroni corrected).

Figure 2. POm encodes whisking activity in absence of reafferent sensory input. (A) The buccal branch of the facial motor nerve was severed unilaterally, preventing whisker motion on the right side

of the face. **(B)** Example POm cell (top, black), ipsilateral (left side of face) whiskers (bottom, blue), and contralateral whiskers (*bottom, gray*). Blue boxes: periods of whisking as in Fig.1B. **(C)** Scatter plot of mean POm firing rate during whisking and quiescence. *Blue*, example cell in B. Firing rates during whisking are significantly higher than quiescence (n = 12 cells from 2 animals, mean increase of 4.8Hz, or 51%, p = 0.00068, paired t test). **(D)** Cross-correlation of POm firing rate and ipsilateral whisking amplitude.

Figure 3. Inhibition of primary motor and somatosensory cortex increases POm correlation with whisking. (A-D) The effect of optogenetic manipulation on thalamic activity. *Left*, bar plots of average firing rates of cells during whisking and quiescence when the laser is off (gray) or on (colored). Right, Cross-correlation of firing rate and whisking amplitude when the laser is off (gray) or on (colored). **(A)** POm recordings during M1 silencing (n = 20 cells, 3 mice. Whisking p = 0.0063, laser p = 0.06, interaction p = 0.038, two-way repeated measures ANOVA). **(B)** POm recordings during S1 silencing (n = 11 cells, 3 animals. Whisking p = 0.0002, laser p = 0.024, interaction = 0.44, two-way repeated measures ANOVA). **(C)** VPM recordings during M1 silencing (n = 13 cells, 2 animals. Whisking p = 0.00018, laser p = 0.26, interaction p = 0.92, two-way repeated measures ANOVA). **(D)** VPM recordings during S1 silencing (n = 8 cells, 2 mice. Whisking p = 0.0009, laser p = 0.1, interaction p = 0.26, two-way repeated measures ANOVA).

Figure 4. POm activity tracks pupil dynamics. (A) Sample recording of POm activity (middle, black) with concurrent ipsilateral pupil diameter (blue, top), median whisker angle (*middle, gray*), and whisking amplitude (green, bottom). **(B)** Cross-correlation of pupil diameter and whisking amplitude (30 recording sessions from 7 animals). **(C)** Cross-correlation of POm firing rate (n = 10 cells from 3 animals) with whisking amplitude (*green*) and pupil diameter (*blue*).

Figure 5. LP activity tracks slow whisker dynamics. (A,B) Sample recordings of two LP cells (black) recorded in bright light **(A)** or low light **(B)**, with corresponding median whisker angle (*gray*) whisking amplitude (green), and pupil diameter (blue or orange). **(C)** Scatter plot of mean firing rate in LP cells during whisking and quiescence. *Blue*, cells recorded in bright light; O*range*, cells recorded in low light (n = 29 cells, 4 animals. Mean increase of 5.04 Hz, 42.6%, $p < 10^{-4}$, paired t-test). **(E)** Cross-correlation of LP firing rate with whisking amplitude (green), median whisker angle (red), and 4-30 Hz bandpass filtered angle (black).

Supplemental Information titles and legends

STAR METHODS

REAGENT or RESOURCE	SOURCE	IDENTIFIER
Experimental Models: Organisms/Strains		
Mouse: Emx1-IRES-Cre	Jackson Laboratories	Stock # 005628
Mouse: Rosa-lox-stop-lox (RSL)-eNpHR3.0/eYFP	Jackson Laboratories	Stock # 014539
Software and Algorithms		

Whisk	Clack *et al.* 2012	https://www.janelia.org/open-science/whisk-whisker-tracking
MClust	A. David Redish, PhD.	http://redishlab.neuroscience.umn.edu/mclust/MClust.html

All experiments complied with the NIH Guide for the Care and Use of Laboratory Animals and were approved by the Institutional Animal Care and Use Committee of Columbia University. Twenty-two C57BL/6 mice were used in these experiments.

Surgery

Mice were anesthetized with isoflurane and placed in a stereotax. The skull was exposed, a thin layer of superglue was applied, and a custom-cut stainless steel headplate was attached using dental acrylic. A small (200 µm wide) opening was made on the mouse's left side at ~1.7 mm posterior to bregma and 1.4 mm lateral of the midline. A silver wire or screw was inserted over the frontal cortex of the same hemisphere as a ground electrode and covered with dental acrylic. The skin was sealed to the implant using superglue. Mice were allowed to recover from surgery for 5 days before habituation. Mice were habituated to the setup for 5 days by attaching their headplate to a holder on the recording table for 5-30 min each day, during which no recordings were performed.

Electrophysiology

After habituation, a mouse would be recorded from for 3-7 days. A glass micropipette (opening ~1.5 µm ID, shank ~60-80 µm OD over last 3-4 mm) was filled with artificial cerebrospinal fluid (aCSF) and inserted vertically into the brain using a micromanipulator. POm cells were typically recorded at microdrive depths of 2800-3600 µm relative to the pia, and LP cells were recorded at depths of 2100-2600 µm relative to pia. Recordings were made with a MultiClamp 700B amplifier (Molecular Devices), bessel filtered 300-10,000 Hz, and digitized at 16 kHz using custom Labview software (ntrode). At the end of some experiments, recording sites were labelled with a glass electrode coated in DiI inserted to a depth of 3600 µm relative to the pia.

Videography

Whisker and pupil videos were made during electrophysiology and imaging using multiple PS3eye cameras running at 125 frames per second. Camera housings had been removed, and the lenses replaced with a 12 mm F2.0 lens (M12 Lenses Inc, part # PT-1220). Video was acquired using the CodeLaboratories PS3eye camera driver and the GUVCView software on linux computer.

Optogenetics

Optogenetic silencing of cortex was performed using Emx1-Halo mice as previously described (Hong *et al.*, 2018) . Briefly, Emx1-IRES-Cre knock-in mice (Jackson Laboratories, stock #005628) were crossed to Rosa-lox-stop-lox (RSL)-eNpHR3.0/eYFP mice (Ai39, JAX, stock# 006364), which express halorhodopsin after excision of a stop cassette by Cre recombinase. All mouse lines were maintained on a C57BL/6 background. Optogenetic experiments used mice that were heterozygous for the desired transgene as assessed by in-house genotyping. The locations of S1 and M1 were marked based on stereotaxic coordinates during headplate surgery, and the skull was thinned before recordings. Light was generated by a 593- or 594-nm laser (OEM or Coherent) coupled to a 200-µm diameter, 0.39 NA optic fiber (Thorlabs) via a fiberport, and the diamond-knife cut fiber tip was placed above M1 or S1.

Nerve Transection

The facial nerve was transected with the mouse under isoflurane anesthesia. A small (~5 mm) incision, centered ~5-8 mm ventral of the eye, was made in the skin. The buccal branch of the facial was identified running from near the ear to the whisker pad, blunt dissected free of underlying tissue, and cut. The skin was closed with stitches and bupivacaine applied.

Histology

At the end of experiments, mice were deeply anesthetized with sodium pentobarbital and then perfused transcardially with 1X phosphate buffer followed by 4% paraformaldehyde. Brains were removed and sectioned on a vibratome into 100µm-thick slices, or on a freezing microtome into 50µm-thick slices. 100-µm slices were mounted directly on glass slides with mounting medium. 50-µm slices were stained in a solution of Cytochrome C (0.3 mg/ml), Catalase (0.4mg/ml), and 3-3'-Diaminobenzidine (DAB, 0.583mg/mL). Sections were incubated in this solution at 40C for 30-45 minutes. Sections were washed 5 times in 1X phosphate buffer and mounted on glass slides with mounting medium.

Data Analysis

Putative action potentials were identified offline with custom MATLAB software. Spikes were then sorted with MClust (version 4.3).

Whiskers were automatically tracked from videos using software (Clack *et al.* 2012). Custom MATLAB software was used to compute the median whisker angle. The median angle was bandpass filtered from 4 to 30 Hz and passed through a Hilbert transform to calculate phase. We defined the upper and lower envelopes of the whisking angle as the points in the whisk cycle where phase equaled 0 (most protracted) or π (most retracted), respectively. Whisking amplitude was defined as the difference between these two envelopes. Periods of whisking and quiescence were defined as times where whisking amplitude exceeded 20% of maximum for at least 250 msec. Periods of time where amplitude exceeded this threshold for less than 250 msec were considered ambiguous and excluded from analysis of whisking vs quiescence.

For each cell, each spike that occurred while the mouse was whisking was assigned a phase. The distribution of possible spike phases (-π to π) was calculated using 32 equally sized bins. Using the same binning, we then calculated the distribution of phases observed in the video to determine the time the whiskers spent at various mean phases. We then normalized the spike phase distribution by the phase distribution to calculate firing rate as a function of phase. The modulation of the cell was characterized by fitting a sine function with a period of 2π to this rate function using least-squares regression. The modulation depth was calculated as the amplitude of the fitted sine wave divided by the cell's mean firing

rate as in (Moore *et al.*, 2015). To test the significance of this modulation, we compared the distributions of phase and (unnormalized, unbinned) spike phase with a Kuiper test and a Bonferroni multiple-comparisons correction.

Pupil diameter was measured from video using custom MATLAB software. Videos were level-adjusted and thresholded to maximize the contrast between the pupil and the rest of the eye. The built in imfindcircles() function was used to locate the pupil and measure diameter on each frame.

References

Audette, N. J. *et al.* (2019) 'Rapid Plasticity of Higher-Order Thalamocortical Inputs during Sensory Learning', *Neuron*. Elsevier, 103(2), pp. 277-291.e4. doi: 10.1016/J.NEURON.2019.04.037.

Chiaia, N. L. *et al.* (1991) 'Thalamic processing of vibrissal information in the rat. I. Afferent input to the medial ventral posterior and posterior nuclei', *The Journal of Comparative Neurology*. Wiley-Blackwell, 314(2), pp. 201–216. doi: 10.1002/cne.903140202.

Constantinople, C. M. and Bruno, R. M. (2011) 'Effects and mechanisms of wakefulness on local cortical networks', *Neuron*. doi: 10.1016/j.neuron.2011.02.040.

Constantinople, C. M. and Bruno, R. M. (2013) 'Deep cortical layers are activated directly by thalamus', *Science*. American Association for the Advancement of Science, 340(6140), pp. 1591–1594. doi: 10.1126/science.1236425.

Diamond, M. E. *et al.* (1992) 'Somatic sensory responses in the rostral sector of the posterior group (POm) and in the ventral posterior medial nucleus (VPM) of the rat thalamus', *Journal of Comparative Neurology*. John Wiley & Sons, Ltd, 318(4), pp. 462–476. doi: 10.1002/cne.903180410.

Diamond, M. E. *et al.* (2008) '"Where" and "what" in the whisker sensorimotor system', *Nature Reviews Neuroscience*. Nature Publishing Group, 9(8), pp. 601–612. doi: 10.1038/nrn2411.

Frangeul, L. *et al.* (2014) 'Specific activation of the paralemniscal pathway during nociception', *European Journal of Neuroscience*, 39(9), pp. 1455–1464. doi: 10.1111/ejn.12524.

Gambino, F. *et al.* (2014) 'Sensory-evoked LTP driven by dendritic plateau potentials in vivo', *Nature*. Nature Publishing Group, 515(7525), pp. 116–119. doi: 10.1038/nature13664.

Guillery, R. W. and Sherman, S. M. (2002) 'Thalamic Relay Functions and Their Role in Corticocortical Communication: Generalizations from the Visual System', *Neuron*. Cell Press, 33(2), pp. 163–175. doi: 10.1016/S0896-6273(01)00582-7.

Herkenham, M. (1980) 'Laminar organization of thalamic projections to the rat neocortex', *Science*. American Association for the Advancement of Science, 207(4430), pp. 532–535. doi: 10.1126/science.7352263.

Hill, D. N. *et al.* (2011) 'Primary Motor Cortex Reports Efferent Control of Vibrissa Motion on Multiple Timescales', *Neuron*, 72(2), pp. 344–356. doi: 10.1016/j.neuron.2011.09.020.

Hong, Y. K. *et al.* (2018) 'Sensation, movement and learning in the absence of barrel cortex', *Nature*. Springer US. doi: 10.1038/s41586-018-0527-y.

Karnath, H., Himmelbach, M. and Rorden, C. (2002) 'The subcortical anatomy of human spatial neglect: putamen, caudate nucleus and pulvinar', *Brain*. Narnia, 125(2), pp. 350–360. doi: 10.1093/brain/awf032.

Masri, R. *et al.* (2006) 'Cholinergic regulation of the posterior medial thalamic nucleus', *Journal of Neurophysiology*. NIH Public Access, 96(5), pp. 2265–2273. doi: 10.1152/jn.00476.2006.

Masri, R. *et al.* (2008) 'Encoding of stimulus frequency and sensor motion in the posterior medial thalamic nucleus', *Journal of Neurophysiology*. American Physiological Society, 100(2), pp. 681–689. doi: 10.1152/jn.01322.2007.

Masri, R. *et al.* (2009) 'Zona incerta: A role in central pain', *Journal of Neurophysiology*. American

Physiological Society, 102(1), pp. 181–191. doi: 10.1152/jn.00152.2009.

Mease, R. A., Metz, M. and Groh, A. (2016) 'Cortical Sensory Responses Are Enhanced by the Higher-Order Thalamus', *Cell Reports*. Elsevier B.V., 14(2), pp. 208–215. doi: 10.1016/j.celrep.2015.12.026.

Meyer, H. S. *et al.* (2010) 'Number and laminar distribution of neurons in a thalamocortical projection column of rat vibrissal cortex', *Cerebral Cortex*, 20(10), pp. 2277–2286. doi: 10.1093/cercor/bhq067.

Moore, C. I. (2004) 'Frequency-Dependent Processing in the Vibrissa Sensory System', *Journal of Neurophysiology*. American Physiological Society, 91(6), pp. 2390–2399. doi: 10.1152/jn.00925.2003.

Moore, J. D. *et al.* (2015) 'Vibrissa Self-Motion and Touch Are Reliably Encoded along the Same Somatosensory Pathway from Brainstem through Thalamus.', *PLoS biology*. Public Library of Science, 13(9), p. e1002253. doi: 10.1371/journal.pbio.1002253.

Nakamura, H. *et al.* (2015) 'Different cortical projections from three subdivisions of the rat lateral posterior thalamic nucleus: A single-neuron tracing study with viral vectors', *European Journal of Neuroscience*. John Wiley & Sons, Ltd (10.1111), 41(10), pp. 1294–1310. doi: 10.1111/ejn.12882.

Olsen, G. M. and Witter, M. P. (2016) 'Posterior parietal cortex of the rat: Architectural delineation and thalamic differentiation', *Journal of Comparative Neurology*. John Wiley & Sons, Ltd, 524(18), pp. 3774–3809. doi: 10.1002/cne.24032.

Petersen, S. E., Robinson, D. L. and Keys, W. (1985) 'Pulvinar nuclei of the behaving rhesus monkey: visual responses and their modulation.', *Journal of neurophysiology*. American Physiological Society Bethesda, MD , 54(4), pp. 867–86. doi: 10.1152/jn.1985.54.4.867.

Petersen, S. E., Robinson, D. L. and Morris, J. D. (1987) 'Contributions of the pulvinar to visual spatial attention.', *Neuropsychologia*, 25(1A), pp. 97–105. Available at: http://www.ncbi.nlm.nih.gov/pubmed/3574654 (Accessed: 17 July 2019).

Phillips, J. W. *et al.* (2019) 'A repeated molecular architecture across thalamic pathways', *Nature Neuroscience*. Springer US, 22(11), pp. 1925–1935. doi: 10.1038/s41593-019-0483-3.

Pinault, D. and Deschênes, M. (1998) 'Projection and innervation patterns of individual thalamic reticular axons in the thalamus of the adult rat: A three-dimensional, graphic, and morphometric analysis', *Journal of Comparative Neurology*. John Wiley & Sons, Ltd, 391(2), pp. 180–203. doi: 10.1002/(SICI)1096-9861(19980209)391:2<180::AID-CNE3>3.0.CO;2-Z.

Poulet, J. F. A. F. A. *et al.* (2012) 'Thalamic control of cortical states', *Nature Neuroscience*. Nature Publishing Group, 15(3), pp. 370–372. doi: 10.1038/nn.3035.

Poulet, J. F. A. F. A. and Petersen, C. C. H. C. H. (2008) 'Internal brain state regulates membrane potential synchrony in barrel cortex of behaving mice', *Nature*, 454(7206), pp. 881–885. doi: 10.1038/nature07150.

Reimer, J. *et al.* (2014) 'Pupil Fluctuations Track Fast Switching of Cortical States during Quiet Wakefulness', *Neuron*. Cell Press, 84(2), pp. 355–362. doi: 10.1016/J.NEURON.2014.09.033.

Reimer, J. *et al.* (2016) 'Pupil fluctuations track rapid changes in adrenergic and cholinergic activity in cortex', *Nature Communications*. Nature Publishing Group, 7. doi: 10.1038/ncomms13289.

Roth, M. M. *et al.* (2016) 'Thalamic nuclei convey diverse contextual information to layer 1 of visual cortex', *Nature Neuroscience*. Nature Publishing Group, 19(2), pp. 299–307. doi: 10.1038/nn.4197.

Saalmann, Y. B. *et al.* (2012) 'The pulvinar regulates information transmission between cortical areas based on attention demands.', *Science (New York, N.Y.)*. American Association for the Advancement of Science, 337(6095), pp. 753–6. doi: 10.1126/science.1223082.

Sherman, S. M. (2016) 'Thalamus plays a central role in ongoing cortical functioning', *Nature Neuroscience*, 19(4), pp. 533–541. doi: 10.1038/nn.4269.

Sherman, S. Murray and Guillery, R. W. (2002) 'The role of the thalamus in the flow of information to the cortex', *Philosophical Transactions of the Royal Society of London. Series B: Biological Sciences*. Edited by P. Adams et al. The Royal Society, 357(1428), pp. 1695–1708. doi: 10.1098/rstb.2002.1161.

Snow, J. C. *et al.* (2009) 'Impaired attentional selection following lesions to human pulvinar: evidence for homology between human and monkey.', *Proceedings of the National Academy of Sciences of the United States of America*. National Academy of Sciences, 106(10), pp. 4054–9. doi: 10.1073/pnas.0810086106.

Trageser, J. C. and Keller, A. (2004) 'Reducing the uncertainty: Gating of peripheral inputs by zona incerta', *Journal of Neuroscience*. Society for Neuroscience, 24(40), pp. 8911–8915. doi: 10.1523/JNEUROSCI.3218-04.2004.

Urbain, N. *et al.* (2015) 'Whisking-Related Changes in Neuronal Firing and Membrane Potential Dynamics in the Somatosensory Thalamus of Awake Mice', *Cell Reports*. The Authors, 13(4), pp. 647–656. doi: 10.1016/j.celrep.2015.09.029.

Varela, C. (2014) 'Thalamic neuromodulation and its implications for executive networks', *Frontiers in Neural Circuits*. Frontiers Media SA. doi: 10.3389/fncir.2014.00069.

Vinck, M. *et al.* (2015) 'Arousal and Locomotion Make Distinct Contributions to Cortical Activity Patterns and Visual Encoding', *Neuron*. Elsevier Inc., 86(3), pp. 740–754. doi: 10.1016/j.neuron.2015.03.028.

Ward, R. *et al.* (2002) 'Deficits in spatial coding and feature binding following damage to spatiotopic maps in the human pulvinar', *Nature Neuroscience*. doi: 10.1038/nn794.

Wilke, M. *et al.* (2010) 'Pulvinar inactivation disrupts selection of movement plans.', *The Journal of neuroscience : the official journal of the Society for Neuroscience*. Society for Neuroscience, 30(25), pp. 8650–9. doi: 10.1523/JNEUROSCI.0953-10.2010.

Williams, L. E. and Holtmaat, A. (2019) 'Higher-Order Thalamocortical Inputs Gate Synaptic Long-Term Potentiation via Disinhibition', *Neuron*. Cell Press, 101(1), pp. 91-102.e4. doi: 10.1016/j.neuron.2018.10.049.

Wimmer, V. C. *et al.* (2010) 'Dimensions of a Projection Column and Architecture of VPM and POm Axons in Rat Vibrissal Cortex', *Cerebral Cortex*. Narnia, 20(10), pp. 2265–2276. doi: 10.1093/cercor/bhq068.

Yu, C. *et al.* (2006) 'Parallel Thalamic Pathways for Whisking and Touch Signals in the Rat', *PLoS Biology*. Public Library of Science, 4(5). doi: 10.1371/journal.pbio.0040124.

Zhang, W. and Bruno, R. M. (2019) 'High-order thalamic inputs to primary somatosensory cortex are stronger and longer lasting than cortical inputs', *eLife*. eLife Sciences Publications Ltd, 8. doi: 10.7554/eLife.44158.

Figure 1. POm cells mainly track slow components of whisking activity

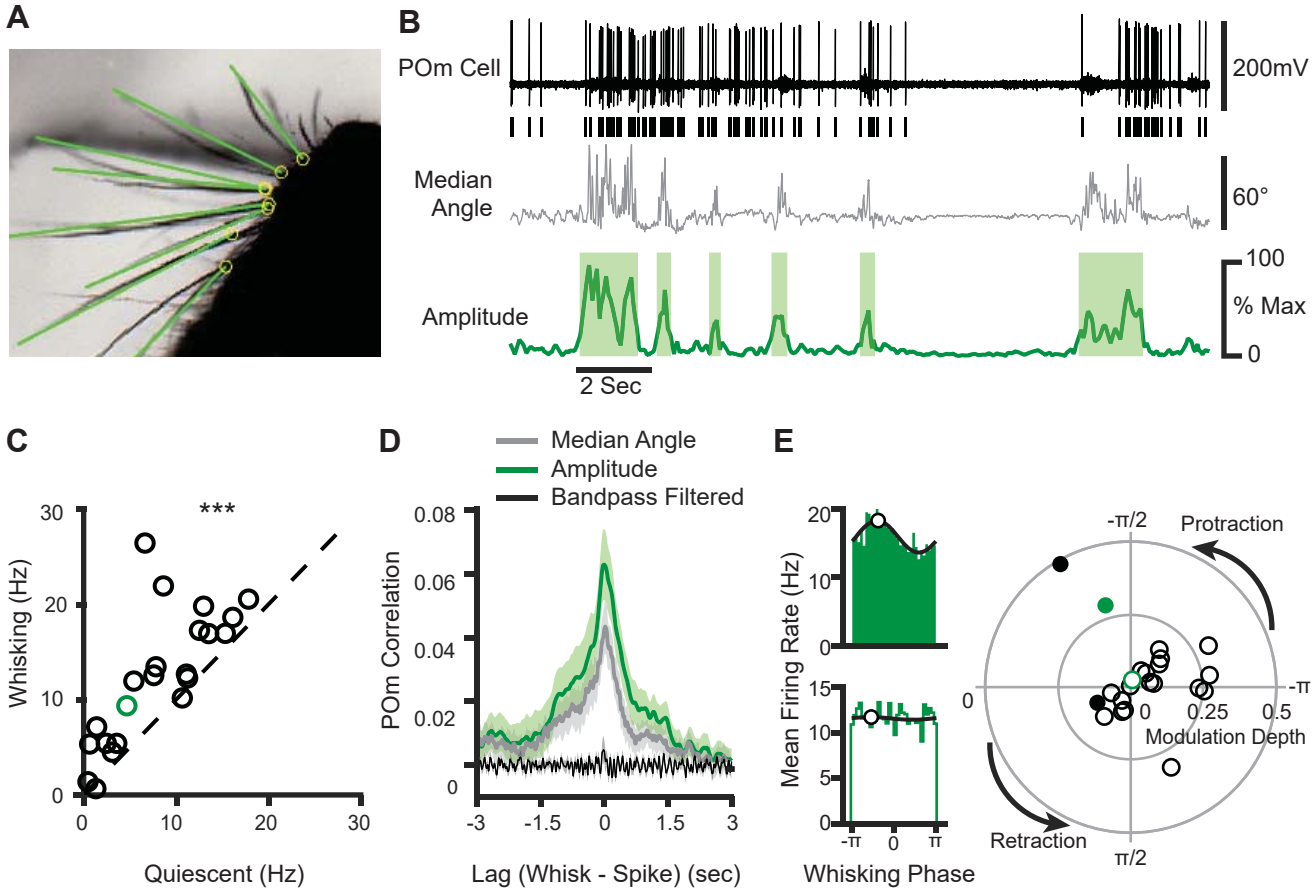

Figure 2. POm encodes whisking in absence of reafferent sensory input.

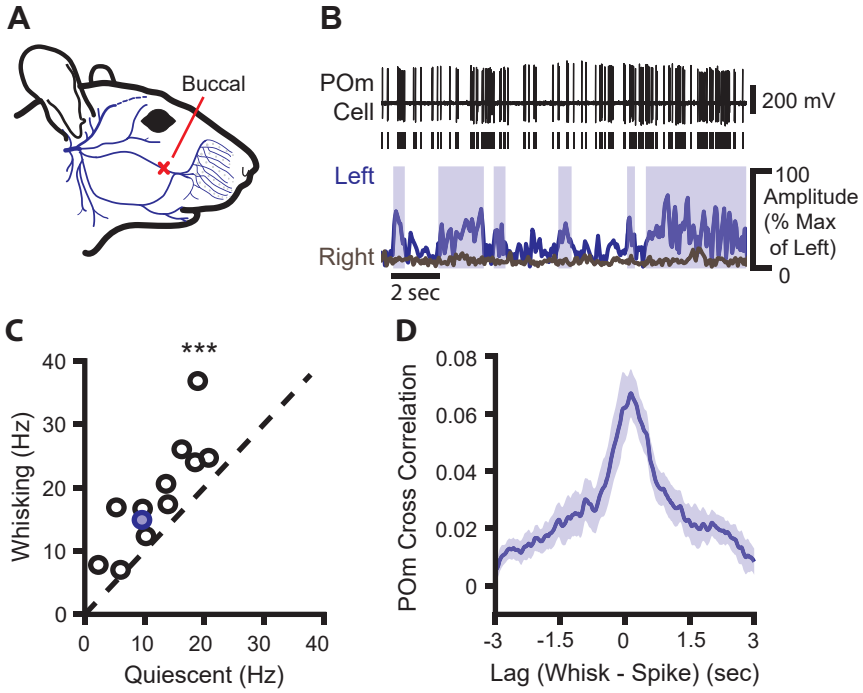

Figure 3. Inhibition of primary motor and somatosensory cortex increases POm correlation with whisking.

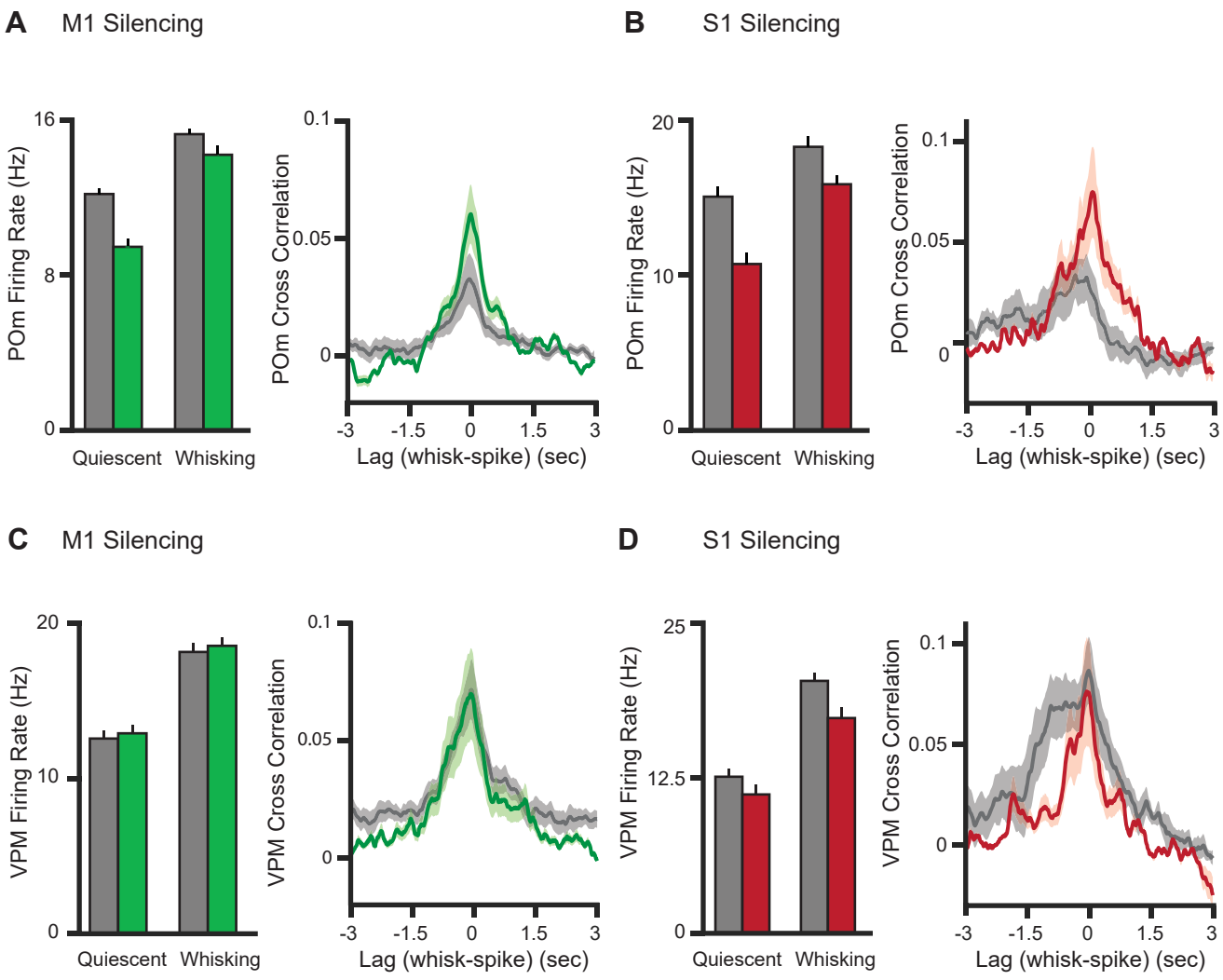

Figure 4: POm activity tracks pupil dynamics

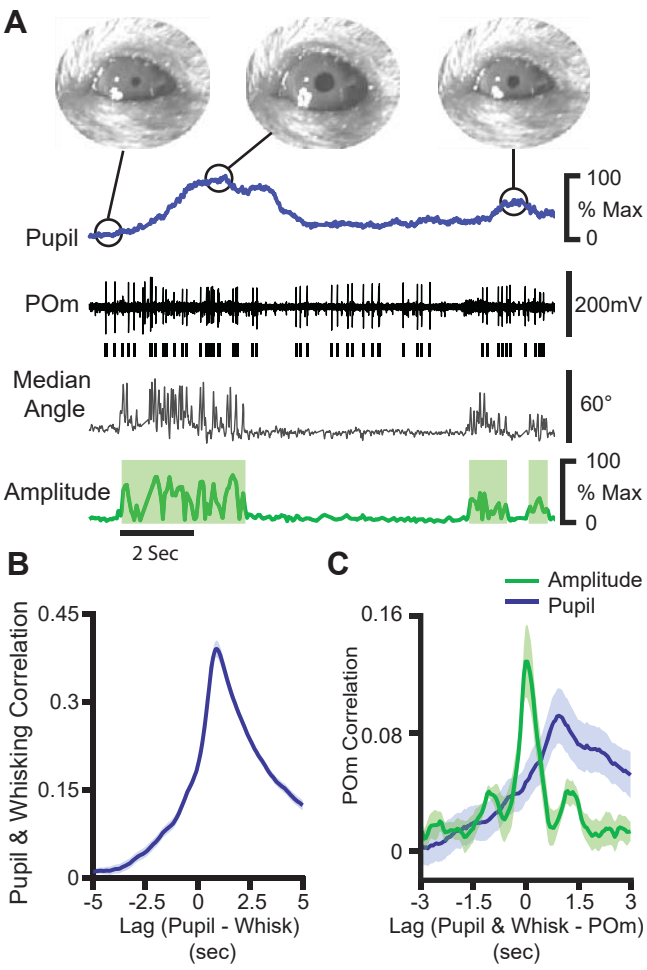

Figure 5: LP activity tracks slow whisker dynamics.